ELSEVIER

www.elsevier.nl/locate/carres

Carbohydrate Research 323 (2000) 147–155

CARBOHYDRATE RESEARCH

The use of NMR residual dipolar couplings in aqueous dilute liquid crystalline medium for conformational studies of complex oligosaccharides

Manuel Martin-Pastor, C. Allen Bush *

Department of Chemistry and Biochemistry, University of Maryland-Baltimore County, Baltimore, MD 21250, USA

Received 18 June 1999; accepted 11 August 1999

Abstract

C–H dipolar coupling values were measured for a natural-abundance sample of the pentasaccharide β-D-Gal*p*-(1→3)-[α-L-Fuc*p*-(1→4)]-β-D-GlcNAc*p*-(1→3)-β-D-Gal*p*-(1→4)-β-D-Glc*p* ('lacto-*N*-fucopentaose 2') (LNF-2), in a 7.5% solution of dimyristoyl phosphatidylcholine–dihexanoyl phosphatidylcholine bicelle liquid crystals oriented in the NMR magnetic field. Interpretation of the dipolar coupling data and NOE confirms the conformational model for the Lewis[a] trisaccharide epitope based on NOE, molecular dynamics simulations, and scalar coupling data and provided new structural information for the remaining residues of the pentasaccharide. Since residual dipolar coupling provides information on long-range order, it is a valuable complement to other types of NMR data such as NOE and scalar coupling for exploring conformations of complex oligosaccharides.

Keywords: Bicelles; Dipolar coupling; Oligosaccharide; Conformation; NMR; Liquid crystal

1. Introduction

Most previous investigations of the conformation of complex oligosaccharides in solution have employed measurements of nuclear Overhauser effect (NOE) in NMR spectroscopy in combination with computer molecular modeling [1–4]. While this approach has proved reasonably effective for relatively rigid oligosaccharides, its shortcomings with more flexible oligosaccharides have stimulated a search for new NMR methods such as ^{13}C scalar coupling [5–8]. Aubin and Prestegard [9] have explored methods that rely on dipolar couplings measured for glycolipids oriented as a result of their attachment to a magnetically oriented liquid crystal. Tjandra and Bax [10] have recently shown that orientation of small proteins can be conveniently achieved in such phospholipid bilayers known as bicelles when the protein is not anchored but is oriented by hydrodynamic interaction. Bolon and Prestegard [11], demonstrating that such bicelles can be used to orient oligosaccharides, reported H–H dipolar coupling effects but not quantitative measurements or an interpretation in terms of a conformational model. Recently, Kiddle and Homans [12] have measured and interpreted C–H dipolar couplings for a ^{13}C-enriched trisaccharide,

Abbreviations: NOE, nuclear Overhauser effect; DMPC, dimyristoyl phosphatidylcholine; DHPC, dihexanoyl phosphatidylcholine; LNF-2, 'lacto-*N*-fucopentaose 2'; HSQC, heteronuclear single quantum coherence.

* Corresponding author. Tel.: +1-410-455-2506; fax: +1-410-455-2608.

E-mail address: bush@umbc.edu (C.A. Bush)

0008-6215/00/$ - see front matter
PII: S0008-6215(99)00237-2

fitting the data to a simulated annealing calculation, and Rundlöf et al. [13] have reported C–H dipolar coupling data for the milk tetrasaccharide, lacto-*N*-*neo*-tetraose (LNnT) in natural abundance. We report here orientation of a milk pentasaccharide 'lacto-*N*-fucopentaose 2' (LNF-2) (see Structure 1), in a dilute bicelle solution of dimyristoyl phosphatidylcholine (DMPC) and dihexanoyl phosphatidylcholine (DHPC) and measurement of C–H dipolar coupling values. In contrast to LNnT, which has a type 2 core structure, LNF-2 has a type 1 core as well as a Lewis[a] trisaccharide epitope that has been proposed to have a single rigid conformation. The dipolar couplings were consistent with the conformation for the Lewis[a] trisaccharide epitope of this oligosaccharide, proposed on the basis of NOE data and long-range H–C scalar coupling constants. Additional information on the conformation of the other two residues of the pentasaccharide was deduced from the dipolar coupling data.

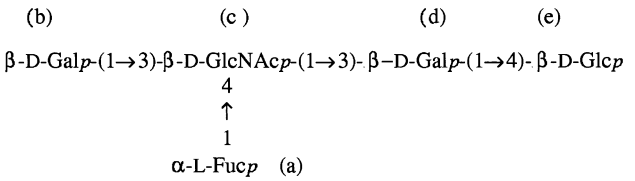

(Structure 1)

2. Experimental

NOE data for LNF-2 were taken from Ref. [14]. The 500-MHz 2D-NOESY spectrum reported there was reanalyzed in order to obtain NOE information concerning residues c, d and e of LNF-2 not previously reported.

A $\sim$15% stock solution in D_2O of DMPC-DHPC in molar ratio of 3:1 was prepared in 30 mM phosphate buffer at pH 7 and mixed by vortexing in several cycles of heating to 40 °C and cooling on ice over a period of 20 h. An LNF-2 solution ($\sim$10 mM) was prepared in an NMR tube by mixing 0.25 mL of the solution of LNF-2 in D_2O with 0.25 mL of the stock bicelle solution. This sample was homogenized by vortexing in several cycles of heating to 40 °C and cooling on ice.

Dipolar coupling values, $^1D_{CH}$, were measured from the difference in the splitting of two t_1-coupled, t_2-decoupled gradient HSQC spectra [15] acquired on a GE-Omega PSG 500 NMR instrument at 35 and 19 °C, corresponding to the oriented and isotropic solution, respectively. In order to maximize the resolution in the indirect dimension, two sets of t_1-folded experiments were acquired, one with ^{13}C carrier position in the center of the anomeric region and the other in the center of the ring region ($\sim$75 ppm). Using this protocol, the linewidth in the t_1 dimension at half height was $\sim$12 Hz (Fig. 1). Since the chemical shifts in the bicelle solution were very similar to those previously reported, the C–H cross-peaks were assigned using the data of Xu et al. [16]. The column corresponding to each C–H signal of LNF-2 was carefully phased and stored. After an inverse Hilbert transformation and zero filling to 16K, the retransformed spectrum showed a digital resolution of 0.2 Hz/pt. Vectors from the 35 °C spectrum were compared with the corresponding vector from the 19 °C spectrum, and the offset required for superposition of the multiplet components was used to calculate the sign and magnitude of $^1D_{CH}$. The experiments were repeated twice and $^1D_{CH}$ couplings averaged. The estimated error is $\pm$0.5 Hz, a figure that is consistent with the error reported by Tjandra et al. [17] for coupling values for bonded N–H pairs in proteins.

Given a geometric model for the molecule, the experimental C–H dipolar coupling values can be interpreted by orienting the molecular alignment tensor A, which can be decomposed into an axially symmetric, A_a and a rhombic component, A_r [10]. The dipolar coupling between two nuclei, C and H is given by

$$^1D_{CH}(\theta,\phi) = S^2\frac{\mu_0}{4\pi}\gamma_C\gamma_H h\left[A_a(3\cos^2\theta-1) + \frac{3}{2}A_r\sin^2\theta\cos^2\phi\right]/4\pi^2 r_{CH}^3 \quad (1)$$

where S^2 is the generalized order parameter for internal motions of the C–H pair [18], μ_0 is the magnetic permeability of vacuum, γ_C and γ_H are the magnetogyric ratios of C and H, h is Planck's constant, r_{CH} is the distance between C and H, and θ and ϕ are cylindrical

coordinates describing the orientation of the C–H vector with respect to the principal axis system of A. While the magnitude and orientation of A are not known, they can be determined by iterative fitting to the measured dipolar couplings for a known structure if S^2 and r_{CH}^3 are known [10].

For the orientation of A, two methods were evaluated. In the first, A is assumed to be axially symmetric and A_r is set equal to zero, resulting in a four-parameter model if S^2 and r_{CH} are assumed identical for all C–H bonds [17]. In the second method, the assumption of axial symmetry was relaxed, leading to a five-parameter fit [17]. In the algorithm used, the direction cosines of the bond vectors are calculated from the Cartesian coordinates of the model molecular structure. For some trial values of the Euler angles (θ, ϕ, ψ) that define the orientation of A, either one parameter A_a (method 1) or two parameters A_a and A_r (method 2) must be calculated to define the alignment tensor A. The goodness of the parameters is then evaluated by the merit function χ^2 defined in Eq. (2):

$$\chi^2 = \frac{\sum_1^n ({}^1D_{CH}^{exp} - {}^1D_{CH}^{calc})^2}{\sum_1^n ({}^1D_{CH}^{exp})^2} \quad (2)$$

In this equation n is the number of C–H dipolar vectors.

A Powell algorithm was used to minimize the merit function and to obtain the optimized Euler angles and the magnitude of A. The optimization was repeated for 10 random starting values of the parameters. Only the parameters corresponding to the lowest χ^2 are reported in Table 1. These parameters were obtained for several different starting values.

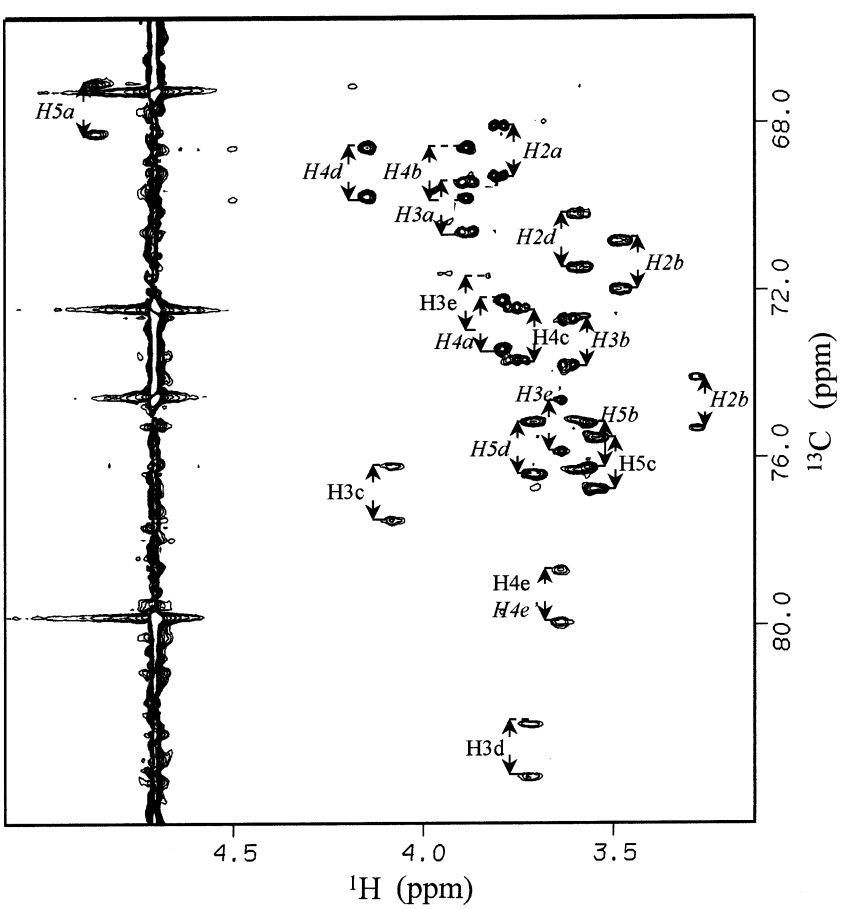

Fig. 1. t_1-Coupled, t_2-decoupled gradient HSQC of LNF-2 oriented in the liquid crystal phase at 35 °C. The carrier was set in the center of the ring region (~ 75 ppm) and the spectral width was 4329 Hz. A matrix of 1024 × 256 data points was acquired for the direct and indirect dimensions, respectively, and was apodized by a 90° shifted sine bell function for the direct dimension. For the t_1 dimension 64 additional points were linearly predicted followed by a 90° shifted sine bell apodization function. Before Fourier transformation in both dimensions, the matrix was zero filled to 1024 × 1024 points.

Table 1
Experimental and calculated dipolar couplings for LNF-2 for conformers found during the different relaxed conformational searches as described in the text

Atom pairs	Conf. 1 [a] $^1D_{CH}^{calc.}$ $\chi^2 = 0.307$	Conf. 2 [b] $^1D_{CH}^{calc.}$ $\chi^2 = 0.134$	Conf. 3 [c] $^1D_{CH}^{calc.}$ $\chi^2 = 0.131$	Conf. 4 [d] $^1D_{CH}^{calc.}$ $\chi^2 = 0.318$	$^1D_{CH}^{exp.}$
H-1–C-1a	1.7	2.0	2.1	2.0	1.8
H-2–C-2a	−2.7	−2.1	−2.0	−2.1	−1.3
H-3–C-3a	−0.9	−0.5	−0.5	−0.5	−0.8
H-4–C-4a	0.2	0.2	0.3	0.2	0.3
H-1–C-1b	−5.2	−5.5	−5.6	−5.6	−5.5
H-2–C-2b	−3.3	−3.5	−3.5	−3.6	−3.2
H-3–C-3b	−4.7	−4.9	−4.9	−5.0	−4.8
H-4–C-4b	6.5	5.9	5.6	6.0	5.8
H-5–C-5b	−4.5	−4.9	−5.0	−5.1	−5.8
H-2–C-2c	11.4	11.6	11.6	11.7	12.1
H-3–C-3c	11.9	12.2	12.0	12.3	11.9
H-4–C-4c	11.3	11.0	11.1	11.1	10.3
H-5–C-5c	11.1	11.2	11.3	11.3	11.5
H-1–C-1d				13.1	12.5
H-2–C-2d				13.1	13.7
H-3–C-3d				13.5	15.3
H-4–C-4d				−2.6	−2.6
H-5–C-5d				13.3	12.4
H-3–C-3e				6.3	6.3
H-4–C-4e				8.3	8.2

[a] Residues a–(b)–c aligned with method 1. ϕ_{ac}/ψ_{ac}: −71.0/142.5, ϕ_{bc}/ψ_{bc}: −72.0/−103.0 (conformer reported in Ref. [19]).
[b] Residues a–(b)–c aligned with method 1. ϕ_{ac}/ψ_{ac} −63.0°/130.8°, ϕ_{bc}/ψ_{bc}: −61.1°/−100.8°.
[c] Residues a–(b)–c aligned with method 2. ϕ_{ac}/ψ_{ac}: −65.4/130.9, ϕ_{bc}/ψ_{bc}: −61.0/−103.1.
[d] All residues aligned with method 1. ϕ_{ac}/ψ_{ac}: −63.0°/130.8°, ϕ_{bc}/ψ_{bc}: −61.1°/−100.8°, ϕ_{cd}/ψ_{cd}: −104.9°/−142.7°, ϕ_{de}/ψ_{de}: −135.1°/94.9°.

In the molecular modeling, the glycosidic dihedral angles are defined according to the IUPAC heavy-atom convention in which ϕ: O-5–C-1–O-1–C-x and ψ: C-$x-1$–C-x–O-1–C-1. Both rigid and relaxed energy conformational maps were performed for the different glycosidic linkages of LNF-2 using InsightII/Discover software (Biosym Technologies, San Diego, CA, USA). For the relaxed energy maps, the glycosidic dihedral angles were restrained by using a cosine type potential with a force constant of 100 kcal mol^{-1}. Each structure was minimized using the CVFF [22] force field and a distance-dependent dielectric of 80*r.

3. Results and discussion

Couplings measured in the indirect dimension (Fig. 1) have the advantage over those measured in the direct (proton) dimension that proton dipolar coupling does not interfere with determination of the C–H coupling values. Without the interference of some large D_{HH} couplings, many more C–H coupling constants can be reliably measured than is possible with the method described by Rundlöf et al. [13]. By optimizing the sweep width in the indirect dimension, rather symmetric line shapes of about 12 Hz width can be obtained, and the precision in the coupling values approaches 0.5 Hz. Although the effect of orientation on ^{15}N chemical shift has been observed in proteins, the effect in ^{13}C should be less due to the smaller chemical shift anisotropy. A small shift in the center of the doublet is not expected to influence the measured value of the splitting.

The Lewis[a] epitope, which is comprised of the three non-reducing terminal residues a, b and c of Structure 1, has been proposed to adopt a single relatively rigid conformation [14,19–21]. Of the 13 dipolar couplings listed for these three residues in Table 1, only five are expected to give truly independent information needed for orientation of the tensor A.

In the normal chair conformation of a pyranoside, axial C–H bond vectors are expected to be essentially parallel. Thus, for β-GlcNAc (c) all the coupling values are approximately 11 ± 1 Hz. α-Fuc (a) has equatorial C–H bonds at C-1 and C-4 that are parallel, yielding two independent vector directions for this residue as is also the case for β-Gal (b).

Conformation 1 (Conf. 1) for the Lewis[a] trisaccharide (a–b–c) component of LNF-2 was built from the glycosidic dihedral angles previously reported [21], in which $\phi_{ac}/\psi_{ac} = -71°/142.5°$ for the Fuc-GlcNAc linkage and $\phi_{bc}/\psi_{bc} = -72°/-103°$ for the Gal-GlcNAc linkage [21]. The three interglycosidic distances H-1a–H-4c, H-5a–H-2b and H-1b–H-3c in this model are in quantitative agreement with the ^{1}H NOE data [14]; the model is also in agreement with C–H scalar coupling constants [16] and molecular dynamics simulations [21]. The results in Table 1 show that this model can be oriented to reproduce the 13 experimental couplings using the first method with a four-parameter orientation function. The discrepancies between experimental and simulated data are slightly beyond the estimated experimental error.

Since the estimated precision of the dihedral angles in the NOE-based model is $\pm 10°$ [14], a refinement of the model with the experimental dipolar coupling data was attempted to determine whether the dipolar coupling data could be used to improve the precision of the model. A relaxed energy grid map was generated for the trisaccharide a–b–c, in which the dihedral angles were varied over the range: ϕ_{ac} (-80 to $-60°$), ψ_{ac} (130 to 150°), ϕ_{bc} (-80 to $-60°$) and ψ_{bc} (-110 to $-90°$) using a grid step of 2.5°. At every ϕ/ψ point the structure was optimized by energy minimization and then aligned by method 1. The conformer that is best able to explain the dipolar couplings and qualitatively the aforementioned interglycosidic NOE distances (< 3.5 Å) of residues a–b–c is Conf. 2 (Table 1). The fitting of the model to the experimental dipolar coupling data is slightly improved, and the glycosidic angles differ only slightly from those of Conf. 1.

In order to test the assumption of an axially symmetric orientation tensor, A, the conformations found in the local relaxed grid search were also aligned using method 2, which fits to five orientation parameters. The best conformation (Conf. 3 in Table 1) has glycosidic dihedral angles very similar to those of Confs. 1 and 2 and a χ^2 only slightly lower than that with the four-parameter fit of method 1. It appears that, at least for this oligosaccharide, an axially symmetric orientation tensor is adequate.

Having concluded that it is possible to orient a model determined from other NMR data, we can ask how good a model can be uniquely determined from C–H dipolar coupling data and just how many independent vectors are required. Since we do not expect that an axially symmetric orientation tensor will be generally applicable, we anticipate that at least four or five independent C–H vectors will be needed to fit the orientation tensor to a correct model. To test the uniqueness, a rigid map was generated for the disaccharide a–c by rotating the dihedral angles ϕ_{ac} and ψ_{ac} from 180 to 180° in 15° steps, while torsions ϕ_{bc} and ψ_{bc} were fixed at -60 and $-100°$, respectively. A map was generated for the disaccharide b–c by rotating ϕ_{bc} and ψ_{bc} from -180 to $-180°$ in 15° steps, while torsions ϕ_{ac} and ψ_{ac} were fixed at -62.5 and 130°, respectively. The 25 conformations that could be oriented with the lowest χ^2 are represented as points in the 'dipolar maps' of Fig. 2.

In the dipolar map generated for the a–c linkage (Fig. 2(a)), the eight dipolar coupling values measured for these two residues were used for tensor alignment. Of the three possible regions that explain the dipolar couplings, only the most extended region with angles around ϕ_{ac}/ψ_{ac}: $-60°/100°$ has interglycosidic distances in qualitative agreement (< 3.5 Å) with the three aforementioned interglycosidic NOEs for residues a–b–c, scalar coupling and molecular modeling. The dipolar map generated by including all the 13 dipolar couplings of the three residues a–b–c (Fig. 2(c)) shows many fewer allowed conformations, although a few lie outside the region of agreement with the other data. A dipolar map generated for the b–c linkage by including only the nine dipolar couplings measured for these two residues (Fig. 2(b)) shows two main regions of agreement, only one of which, with angles

around ϕ_{bc}/ψ_{bc}: $-60°/-100°$, is in qualitative agreement with the interglycosidic NOE data. The dipolar map generated by including all the 13 dipolar couplings of residues a–b–c for the tensor alignment (Fig. 2(d)) shows a more concentrated distribution of the points around the values of Conf. 2, as a result of including four extra vectors for the tensor alignment. The dipolar maps of Fig. 2(c) and (d) combined with the interglycosidic NOE data [14], reduce substantially the uncertainty of the structure due to either flexibility or looseness of the structural restraints for residues a–(b)–c. Not included in these rigid maps is the possible existence of bad steric interactions for some combinations of dihedral angles. Inclusion of a regular molecular mechanics force field further restricts the space for potential flexibility. The combination of the 13 dipolar coupling values, determining five independent directions, provides excellent agreement with the NOE and molecular modeling results for the Lewis[a] trisaccharide epitope having a single conformation given by model 2 or 3 with a precision in glycosidic dihedral angles on the order of 5°.

Given the excellent agreement of the rigid trisaccharide model with the data, the orientation tensor derived for that fragment can be used to interpret the dipolar coupling data for the other two residues of the pentasaccharide. While investigations of the lactose linkage (d–e) have indicated it to be flexible [23,24], it need not be so in the pentasaccharide, and the conformation and flexibility of the β-(1→3) linkage between GlcNAc (c) and Gal (d) has not been established. The NOESY spectrum of LNF-2 [14] showed two interglycosidic NOEs for residues c–d, a strong NOE for H-1c–H-3d and a medium-size NOE for H-1c–H-4d. The presence of these two NOEs is not enough to characterize whether there is

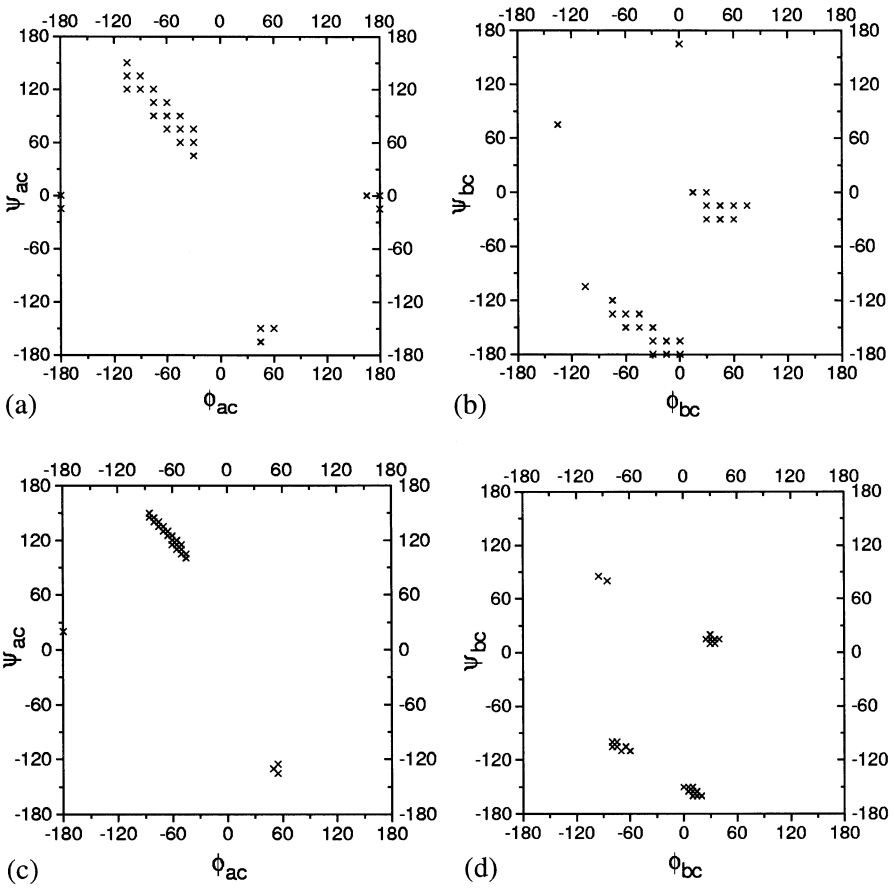

Fig. 2. Dipolar maps representing rigid conformational searches for the Lewis[a] trisaccharide of LNF-2. Only the best 25 structures with smallest χ^2 are plotted. (a) Disaccharide a–c, eight dipolar couplings, χ^2 from 0.17 to 0.22. (b) Disaccharide b–c, nine dipolar couplings, χ^2 from 0.15 to 0.22. (c) Trisaccharide a–b–c, 13 dipolar couplings ϕ_o2/ψ_o2: $-72.5°/-100.0°$, χ^2 from 0.20 to 0.32. (d) Trisaccharide a–b–c, 13 dipolar couplings, ϕ_o1/ψ_o1: $-72.5°/140.0°$, χ^2 from 0.20 to 0.29.

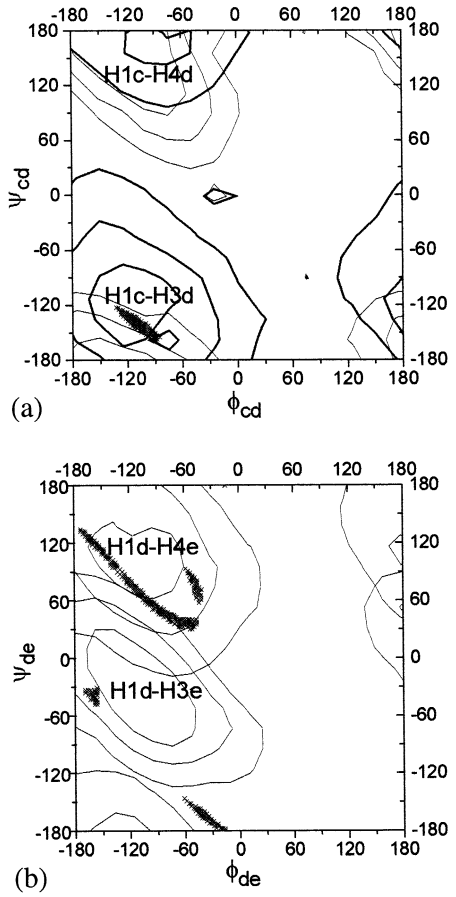

Fig. 3. Dipolar map (crosses) for different linkages of LNF-2 superposed with inter-residual NOE distance contours (lines). The distance contours represented are 2.5, 3.0 and 3.5 Å. (a) Dipolar map for linkage c–d obtained by using dipolar couplings of residues a–(b)–c–d of LNF-2, χ^2 from 0.29 to 0.39. (b) Dipolar map for terminal linkage d–e obtained by using all the dipolar couplings of LNF-2, χ^2 from 0.26 to 0.36.

flexibility or a well-defined conformation for the c–d linkage, since the distance contour map of Fig. 3(a) shows that the ranges of ψ_{cd} between -60 and 120° and ϕ_{cd} between -150 and $-30°$ are compatible with the NOE distance constraints. As will be seen below, the information provided by the $^1D_{CH}$ dipolar couplings can help to solve this ambiguity. A relaxed energy map was generated for the glycosidic torsions of linkage c–d of LNF-2, while maintaining the conformation of residues a–(b)–c fixed in the previously deduced structure, Conf. 2. The glycosidic torsions ϕ_{cd} and ψ_{cd} were rotated from -180 to 180° using a grid step of 2.5°, followed by energy optimization of residues c–d–e. Each conformation resulting from the energy minimization was aligned in order to give the best agreement with the 18 dipolar couplings measured for residues a–(b)–c–d. The dipolar map of Fig. 3(a) summarizes the results in best agreement with the experimental data. It can be seen that all the conformers of the dipolar map are located in a very narrow region of the map near $\phi_{cd} = -100$ and $\psi_{cd} = -140$ in the common region of both interglycosidic NOE distances. The conformer that gave the best agreement with the experimental dipolar couplings is only 0.32 kcal mol^{-1} over the global minimum. The experimental intensities of NOE H-1c–H-3d (s) and NOE H-1c–H-4d (m) are in qualitative agreement (< 3.5 Å) with those expected based on the corresponding proton–proton distances. Although method 1 was used to orient the model, the five-parameter fit (method 2), which accounts for the rhombic term (A_r), gives a similar result.

The conformation of the terminal linkage d–e of LNF-2 was studied using a similar approach and conditions as described for residues c–d. In this case, the previously deduced conformation of residues a–(b)–c–d was fixed, and a ϕ_{de}/ψ_{de} dipolar map was generated. All the dipolar couplings measured for LNF-2 were used for the alignment. The dipolar map of Fig. 3(b) summarizes the conformers in best agreement with the dipolar data. In Fig. 3(b) are also represented the contours of two inter-residue NOEs H-1d–H-4e (s) and H-1d–H-3e (w) obtained for this linkage in the NOESY experiment of LNF-2. In this case, the best agreement with the dipolar couplings (χ^2 0.261) corresponds to a high-energy conformation (data not shown). Conf. 4 (χ^2 0.318) is the first low-energy structure (0.82 kcal mol^{-1} over global minimum) in agreement with dipolar couplings and qualitative agreement with the two interglycosidic NOEs (distance < 3.5 Å). Other low-energy conformers similar to Conf. 4 were found with differences of up to $\pm 5°$ in the glycosidic angles, which gave a similar value of χ^2. The glycosidic angles and calculated dipolar couplings for Conf. 4 with method 1 are given in Table 1, but similar results were obtained with method 2. A stereoview of Conf. 4 is shown in Fig. 4.

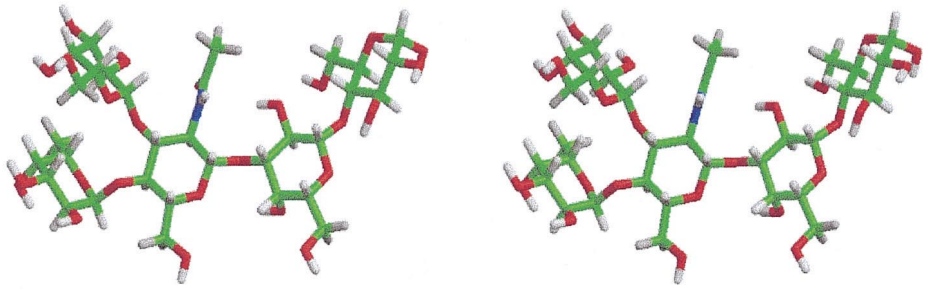

Fig. 4. Stereoview of Conf. 4. ϕ_{ac}/ψ_{ac}: $-63.0°/130.8°$, ϕ_{bc}/ψ_{bc}: $-61.1°/-100.8°$, ϕ_{cd}/ψ_{cd}: $-104.9°/-142.7°$, ϕ_{de}/ψ_{de}: $-135.1°/94.9°$. This conformation agrees with all dipolar couplings and NOE of LNF-2, $\chi^2 = 0.318$.

Previous NMR and molecular mechanics studies of the analogous β-(1→4)-linked disaccharide, lactose, concluded that this molecule exists in a mixture of two major conformations in solution [23,24]. A syn region of the ϕ/ψ map in lactose with angles around $-60°/120°$ is consistent with an exclusive interglycosidic H-1Gal–H-4Glc NOE and an anti region of the ϕ/ψ map with angles around $-60°/-60°$ is consistent with the exclusive interglycosidic H-1Gal—H-3Glc NOE observed [23,24]. The relative populations deduced from quantitative NOE simulation of lactose for syn and anti conformers are ~0.90:0.10, respectively.

In LNF-2, although the interglycosidic NOEs observed for residues d–e [14] are similar to those in lactose, the molecular mechanics optimized distance contours of H-1d–H-4e and H-1d–H-3e of LNF-2 represented in Fig. 3(b) differ slightly from those in lactose. For LNF-2 those contours share a region of the ϕ/ψ map so that they are not exclusive NOEs as they are in lactose [23,24]. This shift in the contours is imposed by steric and electrostatic interactions with the rest of the structure of the oligosaccharide. It is important to notice that the common region of both NOEs in LNF-2 corresponds to a low-energy region of the map in which Conf. 4 is found.

4. Conclusions

C–H dipolar couplings, which can be conveniently measured in natural-abundance oligosaccharides dissolved in phospholipid bicelle solution, can be interpreted if a sufficient number of independent data can be obtained. Not only the quantity but also the quality of C–H vectors is important, since many C–H bonds in pyranosides are essentially parallel. For an oligosaccharide adopting a fixed rigid conformation, at least five independent vector directions such as reported here is likely to be near the minimum number. Depending on the nature and extent of the other conformational information available from NOE, scalar coupling and molecular modeling, the ambiguity of the interpretation can increase rapidly if any of the dipolar coupling data are removed from the fitting procedure. For this pentasaccharide, either a four- or five-parameter fit may be used, but it is quite possible that neglect of the rhombic component, A_r, might not be adequate for other oligosaccharides.

The strategy used here is based on the generation of dipolar maps constructed in a best-fit orientation basis of conformations obtained during a molecular mechanics grid search. The election of the force field is not expected to have an important influence in the conformations deduced because the experimental data are used to select the conformations, while the force field is used to propose them and to reject conformations with severe steric conflicts (i.e., energy >4 kcal mol^{-1} over the global minimum). It is still possible that the use of a different force field could generate slightly different pyranose chair conformations that would affect the orientation of the C–H vectors and would produce a small change in χ^2 and a small shift in the regions represented in the ϕ/ψ dipolar map.

We conclude that the Lewis[a] trisaccharide adopts a single conformation, and the extension of the model for LNF-2 to include the β-GlcNAc-(1→3)-Gal linkage implies that the four residues tumble as a unit with limited

flexibility of the linkages. This result should not be interpreted to imply that the β-GlcNAc-(1→3)-Gal linkage is particularly rigid in all oligosaccharides. Our argument for a fixed conformation for the β-Gal-(1→4)-Glc linkage is less strong, as it relies on only two dipole vectors that are essentially parallel. Since there is some discrepancy between the best dipole orientation and the energy calculations, the angles reported in Table 1 for the d–e linkage may correspond to a virtual conformation. But since coupling values, unlike NOE data, represent simple linear averages, the model is likely to be close to a major conformer, which could differ from that found in lactose.

The combination of both a qualitative analysis of the interglycosidic NOE and the dipolar coupling information was crucial for the structure determination of LNF-2. For a rigid or almost rigid conformation, a consistent interpretation of NOE data and the dipolar coupling can be achieved. Once a model is satisfactorily oriented, other dipolar coupling data such as H–H dipolar coupling [11] can also be interpreted. The existence of a high-amplitude flexibility in a glycosidic linkage, as detected by the existence of incompatible NOEs, precludes or at least limits the use of the dipolar couplings for structural determination. A linear average over the different conformations is required in order to explain the dipolar data, as both the population and the orientation tensor need to be calculated for each structure proposed. For these cases other sources of experimental NMR data, such as long-range C–H and/or C–C dipolar couplings measured in uniformly highly ^{13}C-enriched oligosaccharides [5,8], would be very useful.

We propose that residual dipolar couplings, which can provide information on long-range order, can be a valuable complement to other NMR data such as NOE and scalar coupling, which give information on oligosaccharide conformation over a much shorter range.

Acknowledgements

This research was supported by NSF grant MCB9724133. We thank Dr Nico Tjandra for kindly making available to us the software to perform the orientation of the dipolar coupling vectors. Research supported by NSF Grant MCB9724133.

References

[1] H. van Halbeek, *Curr. Opin. Struct. Biol.*, 4 (1994) 697–709.
[2] S.W. Homans, *Glycobiology*, 3 (1993) 551–555.
[3] T. Peters, B.M. Pinto, *Curr. Opin. Struct. Biol.*, 6 (1996) 710–720.
[4] C.A. Bush, M. Martin-Pastor, A. Imberty, *Ann. Rev. Biophys. Struct. Biol.*, 28 (1999) 269–293.
[5] J.M. Milton, M.A. Harris, M.A. Probert, R.A. Field, S.W. Homans, *Glycobiology*, 8 (1998) 147–153.
[6] Q. Xu, C.A. Bush, *Carbohydr. Res.*, 306 (1998) 335–339.
[7] B. Bose, S. Zhao, R. Stenutz, F. Cloran, F. Bondo, G. Bondo, B. Hertz, I. Carmichael, A. Serianni, *J. Am. Chem. Soc.*, 120 (1998) 11158–11173.
[8] M. Martin-Pastor, C.A. Bush, *Biochemistry*, 38 (1999) 8045–8055.
[9] Y. Aubin, J.H. Prestegard, *Biochemistry*, 32 (1993) 3422–3428.
[10] N. Tjandra, A. Bax, *Science*, 278 (1997) 1111–1114.
[11] P.J. Bolon, J.H. Prestegard, *J. Am. Chem. Soc.*, 120 (1998) 9366–9367.
[12] G.R. Kiddle, S.W. Homans, *FEBS Lett.*, 436 (1998) 128–130.
[13] T. Rundlöf, C. Landersjö, K. Lycknert, A. Maliniak, G. Widmalm, *Magn. Reson. Chem.*, 10 (1998) 773–776.
[14] P. Cagas, C.A. Bush, *Biopolymers*, 30 (1990) 1123–1138.
[15] B.H. John, *J. Magn. Reson. Ser. A*, 101 (1992) 113.
[16] Q. Xu, R. Gitti, C.A. Bush, *Glycobiology*, 6 (1996) 281–288.
[17] N. Tjandra, S. Grzesiek, A. Bax, *J. Am. Chem. Soc.*, 118 (1996) 6264–6272.
[18] G. Lipari, A. Szabo, *J. Am. Chem. Soc.*, 104 (1982) 4546–4559.
[19] R.U. Lemieux, K. Bock, T.J. Delbaere, S. Koto, V.S. Rao, *Can. J. Chem.*, 58 (1980) 631–653.
[20] H. Kogelberg, T.J. Rutherford, *Glycobiology*, 4 (1994) 49–57.
[21] C. Mukhopadhyay, C.A. Bush, *Biopolymers*, 31 (1991) 1737–1746.
[22] A.T. Hagler, P. Lifson, P. Dauber, *J. Am. Chem. Soc.*, 101 (1979) 5122–5130.
[23] J.L. Asensio, J. Jimenez-Barbero, *Biopolymers*, 35 (1995) 55–73.
[24] M. Martin-Pastor, J.F. Espinosa, J.L. Asensio, J. Jimenez-Barbero, *Carbohydr. Res.*, 298 (1997) 15–49.